

## Magnetorheological Behavior of Polyethylene Glycol-Coated Fe<sub>3</sub>O<sub>4</sub> Ferrofluids

Xiuying QIAO<sup>†</sup>, Mingwen BAI<sup>\*</sup>, Ke TAO<sup>\*</sup>, Xinglong GONG<sup>\*\*</sup>, Rui GU<sup>\*\*</sup>,  
Hiroshi WATANABE<sup>\*\*\*</sup>, Kang SUN<sup>\*</sup>, Jingyuan WU<sup>\*</sup>, and Xiaoyu KANG<sup>\*</sup>

<sup>\*</sup>State Key Laboratory of Metal Matrix Composites, Shanghai Jiao Tong University, Shanghai 200240, China

<sup>\*\*</sup>CAS Key Laboratory of Mechanical Behavior and Design of Materials, Department of Modern Mechanics, University of Science and Technology of China, Hefei, Anhui 230027, China

<sup>\*\*\*</sup>Institute of Chemical Research, Kyoto University, Uji, Kyoto 611-0011, Japan

(Received : October 8, 2009)

Polyethylene glycol (PEG)-coated Fe<sub>3</sub>O<sub>4</sub> ferrofluids were prepared by suspending the PEG-coated Fe<sub>3</sub>O<sub>4</sub> nanoparticles in an oligomeric PEG-400 carrier liquid, and their magnetorheological steady flow behavior was investigated. The PEG modification did not change the crystalline structure of Fe<sub>3</sub>O<sub>4</sub>, and the PEG-coated Fe<sub>3</sub>O<sub>4</sub> nanoparticles were of nearly spherical shape and had a narrow size distribution (4±1 nm in diameter). These nanoparticles exhibited no significant aggregation in the absence of the magnetic field. Under the magnetic field, the nanoparticles aggregated into string-like clusters oriented in the direction of the field. Correspondingly, the ferrofluids behaved essentially as the Newtonian fluids in the absence of the magnetic field but exhibited, under the magnetic field, a magnetorheological effect, i.e., the increase of the shear stress/viscosity associated with a pseudo-plastic and thinning character with no real yield stress. This lack of the real yield stress, possibly reflecting the absence of huge clusters connecting the measuring parts (plates) in the rheometer, suggested that the magnetorheological effect of the ferrofluids were related to deformation/disruption of the magnetically formed clusters of finite sizes under the shear. Interestingly, this effect was most significant for the Fe<sub>3</sub>O<sub>4</sub> nanoparticles having an intermediate amount of PEG coating. This result suggested a possibility that the relaxation of PEG chains in the coating layers of nanoparticles in the clusters contributed to the magnetorheological effect.

**Key Words:** PEG-coated Fe<sub>3</sub>O<sub>4</sub> ferrofluid / magnetorheological effect / pseudo-plasticity

### 1. INTRODUCTION

In recent years, ferrofluids (FFs), colloidal suspensions of magnetic nano-ferroparticles stabilized by polymer coating, have attracted a great attention in the biomedical fields related to magnetic resonance imaging (MRI)<sup>1-3</sup>, hyperthermia therapy of cancers<sup>4,5</sup>, and targeted drug delivery.<sup>6,7</sup> A particular interest is placed on the superparamagnetic nano-ferroparticles (with a diameter < 10 nm) of magnetite (Fe<sub>3</sub>O<sub>4</sub>) because of their high magnetic saturation, negligible toxicity, and easier surface modification. On application of a magnetic field, these particles carrying drug or gene can be targeted to a specific site and/or held in the tumour region. This kind of operation can reduce the harm to healthy organs, because the circulation of the drug throughout the body is limited and non-specific uptake by the reticular-endothelial system can be avoided.

For regulation of the physical and chemical properties of the magnetic nanoparticles and enhancement of the stability and hydrophilicity of the magnetic fluids, several biocompatible water-soluble polymers have been used to coat the surface of those nanoparticles. These polymers include dextran<sup>8,9</sup>, poly(ethylene glycol) (PEG)<sup>10-15</sup>, and poly(vinylpyrrolidone) (PVP).<sup>16</sup> In particular, PEG exhibits great predominance with improved biocompatibility, biodegradability and blood circulation times.

Characterization of the rheological properties plays an important role in the molecular design/application of the magnetorheological fluids, because the rheological properties of the fluids such as the apparent viscosity, yield stress, and stiffness can be controlled by an external magnetic field.<sup>17-20</sup> These fluids, including the above-mentioned ferrofluids, typically consist of micron-sized magnetizable solid particles suspended in a nonconducting carrier liquid. Those fluids, behaving as low viscosity Newtonian fluids in the absence of a magnetic field, are converted to highly viscous (and

<sup>†</sup> To whom correspondence should be addressed.  
E-mail: xyqiao@sjtu.edu.cn

solid-like) materials on application of the field thereby being utilized as dampers, clutches and actuators, etc. This magnetorheological change results from organization of the nanoparticles (randomly dispersed in the absence of the magnetic field) into chain-, column-, or more complicatedly-shaped clusters oriented in the field direction.

This paper focuses on three kinds of PEG-coated  $\text{Fe}_3\text{O}_4$  nanoparticles prepared with different amount of PEG to examine their morphology, structure and composition. Furthermore, magnetorheological property is examined for ferrofluids of these nanoparticles dispersed in an oligomeric PEG solvent. It turned out that the ferrofluids behave as pseudo-plastic fluids having no real yield stress under the magnetic field. This behavior of the ferrofluids is discussed in relation to the contribution of PEG coating to the magnetorheological behavior of those fluids.

## 2. EXPERIMENTAL

### 2.1 Materials

Diethylene glycol (99 %) was purchased from Sigma-Aldrich.  $\text{FeCl}_3 \cdot 6\text{H}_2\text{O}$  (> 99 %),  $\text{NaOH}$  (> 96 %), PEG-20000 ( $M_w = 20000$  g/mol, > 99 %), an oligomeric PEG-400 ( $M_w = 400$  g/mol, > 99 %), and acetone (> 99 %) were purchased from Sinopharm Chem Reagent Co. All these chemicals were analytical grade and utilized, without further purification, in preparation of ferrofluids. Milli-Q water was also utilized.

### 2.2 Preparation of PEG-Coated $\text{Fe}_3\text{O}_4$ Nanoparticles

The synthesis of magnetite nanoparticles followed Yin's method<sup>21)</sup> with some modifications. A  $\text{NaOH}/\text{DEG}$  solution was prepared by dissolving 4 g of  $\text{NaOH}$  in 20 ml of diethylene glycol (DEG) and stirring at 400 rpm for 1h at 120 °C under nitrogen protection. Then, the solution was cooled and kept at 80 °C for use. A slightly yellow, transparent  $\text{PEG}/\text{FeCl}_3/\text{DEG}$  solution was separately prepared by dissolving a prescribed mass of PEG-20000 and 0.54 g of  $\text{FeCl}_3$  in 15 ml of DEG and stirring at 400 rpm for 30 min at 200 °C under nitrogen protection. The mass of PEG was chosen to be 0.30 g, 0.45 g, and 0.60 g. On rapid injection of 2 ml of the  $\text{NaOH}/\text{DEG}$  solution into the  $\text{PEG}/\text{FeCl}_3/\text{DEG}$  solution, the solution mixture turned black immediately. This change of the color was indicative of the formation of oxidized  $\text{Fe}_3\text{O}_4$  nanoparticles having the PEG layer physically adsorbed to their surface. This mixture was heated to and kept at 200 °C for 1h to complete the reaction. Differing from the classical method of coprecipitation of ferric and ferrous salts, no ferrous salt was utilized in our method because DEG acted

as not only a solvent but also a reductant partially reducing  $\text{Fe}^{3+}$  to  $\text{Fe}^{2+}$ .<sup>21)</sup> The high reaction temperature in our method gave highly crystalline magnetic nanoparticles with narrow size distribution.

The black magnetic nanoparticles prepared as above were precipitated and washed five times with acetone, collected by magnet adsorption, and then freeze-dried at -45 °C for 24 h. With the use of 0.30 g, 0.45 g, and 0.60 g of PEG in the above reaction, three kinds of PEG-coated  $\text{Fe}_3\text{O}_4$  nanoparticles were obtained. They were designated as 0.30PEG- $\text{Fe}_3\text{O}_4$ , 0.45PEG- $\text{Fe}_3\text{O}_4$ , and 0.60PEG- $\text{Fe}_3\text{O}_4$ , respectively.

### 2.3 Characterization of PEG-Coated $\text{Fe}_3\text{O}_4$ Nanoparticles

A JEOL JEM-2010 transmission electron microscope (TEM) (JEOL, Japan) was used to observe the morphology of PEG-coated  $\text{Fe}_3\text{O}_4$  nanoparticles at an accelerating voltage of 200 KV. Before the TEM observation, each of three series of nanoparticles (having different PEG content) was dispersed in water and drop-wisely cast onto a carbon coated copper grid, and the excess solvent was removed by freeze-drying. For each series, about 500 nanoparticles were observed to determine their average diameter.

Wide-angle X-ray diffraction patterns were obtained at room temperature with a D-MAX 2550 X-ray powder diffractometer (Shimadzu, Japan) equipped with a Ni-filtered  $\text{Cu K}_\alpha$  radiation ( $\text{CuK}_{\alpha 1} = 0.154$  nm) in the reflection mode. All the measurements were made at 40 KV and 40 mA, and the scattering angle  $2\theta$  was scanned from 10° to 90° at a rate of 5°/min.

Fourier transform infrared (FTIR) measurements were carried out with a Perkin-Elmer Paragon 1000 Fourier Transform Infrared Spectrometer (Perkin-Elmer, USA). Disk-shaped specimens were prepared by pressing the uniform mixtures of nanoparticles and KBr, and the FTIR spectra were recorded from 400 to 4500  $\text{cm}^{-1}$  at room temperature.

For characterization of the chemical composition of the PEG-coated  $\text{Fe}_3\text{O}_4$  nanoparticles, a weight loss of these nanoparticles on heating was measured with a TGA2050 Thermogravimetric Analyzer (TA, USA). All measurements were performed from room temperature to 800 °C at a heating rate of 20 °C/min in a nitrogen atmosphere.

### 2.4 Magnetorheological Characterization for ferrofluids of PEG-coated $\text{Fe}_3\text{O}_4$ Nanoparticles

The ferrofluids of the PEG-coated  $\text{Fe}_3\text{O}_4$  nanoparticles were prepared by suspending, with the aid of supersonication, three kinds of nanoparticles, 0.30PEG- $\text{Fe}_3\text{O}_4$ , 0.45PEG- $\text{Fe}_3\text{O}_4$  and 0.60PEG- $\text{Fe}_3\text{O}_4$ , in the solvent (oligomeric PEG-400). The

nanoparticle concentration was 40 mg/ml in all ferrofluids examined. Because of a good compatibility between the PEG-coated nanoparticles and PEG-400 solvent, well-dispersed suspensions were obtained without sedimentation/formation of huge aggregates.

A VHX-200 Digital Microscope (Keyence, Japan) was operated to observe the structure formation under the magnetic field. Before observation, the ferrofluids of PEG-coated Fe<sub>3</sub>O<sub>4</sub> nanoparticles were dropped onto a thin glass sheet. After a clear eyeshot, a magnetic field was applied and photographs were taken to trace the field-induced evolution of the cluster structure.

Magnetorheological behavior of the ferrofluids of the PEG-coated Fe<sub>3</sub>O<sub>4</sub> nanoparticles was examined at room temperature with Physica MCR 301 Rheometer (Anton Parr, Germany) having a magnetorheological device. The parallel-plate fixture of 20 mm diameter was used, and the gap was set at 0.5 mm. During the measurements, the electromagnetic coil was activated with the currents from 0 A to 1.0 A, corresponding to the magnetic flux densities from 0 T to 0.22 T inside the gap. Steady shear experiments were carried out for the ferrofluids at the shear rate ranging from 0.01 to 100 s<sup>-1</sup> and under different magnetic flux densities.

### 3. RESULTS AND DISCUSSION

#### 3.1 Morphology Observation

Fig. 1 shows the TEM image of 0.30PEG-Fe<sub>3</sub>O<sub>4</sub> nanoparticles. These nanoparticles are of nearly spherical shape and have a narrow size distribution (mostly between 3 and 5 nm) with an average diameter of 4 nm. The other nanoparticles, 0.45PEG-

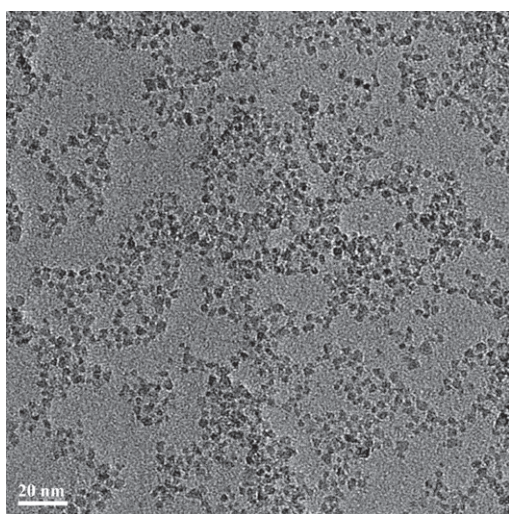


Fig. 1. TEM images of 0.30PEG-coated Fe<sub>3</sub>O<sub>4</sub> nanoparticles. The image was very similar also for 0.45PEG-coated and 0.60PEG-coated Fe<sub>3</sub>O<sub>4</sub> nanoparticles.

Fe<sub>3</sub>O<sub>4</sub> and 0.60PEG-Fe<sub>3</sub>O<sub>4</sub> with different PEG content, had the average size and shape very similar to those of 0.30PEG-Fe<sub>3</sub>O<sub>4</sub> nanoparticles.

Bare Fe<sub>3</sub>O<sub>4</sub> nanoparticles easily form huge aggregates because of their large specific surface area and high surface energy. However, our PEG-coated Fe<sub>3</sub>O<sub>4</sub> nanoparticles hardly formed such aggregates and were well dispersed as seen in Fig. 1, because the PEG coating layer prohibits real close contact of nanoparticles to reduce their mutual attraction.

#### 3.2 Crystalline Structure Analysis

The X-ray diffraction patterns of the three kinds of PEG-coated Fe<sub>3</sub>O<sub>4</sub> nanoparticles are shown in Fig. 2. These patterns detect not only the nanocrystalline structure of the nanoparticles and but also the mean particle size. The PEG-coated Fe<sub>3</sub>O<sub>4</sub> nanoparticles having different amount of PEG coating exhibit similar diffraction peaks characteristic to the standard Fe<sub>3</sub>O<sub>4</sub> cubic crystalline phase at 30.2°, 35.6°, 43.2°, 56.8° and 62.8°; These peaks correspond to the diffraction of the crystalline planes of (220), (311), (400), (511) and (440) respectively. The coincidence of the diffraction patterns of those nanoparticles suggests that the crystalline structure of Fe<sub>3</sub>O<sub>4</sub> did not change on the modification of the particles with PEG chains. This result indicates that the PEG coating occurs only at the Fe<sub>3</sub>O<sub>4</sub> nanoparticle surface and gives no detectable chemical/physical change in bulk of the nanoparticles.<sup>2)</sup>

The crystallite size  $L_{hkl}$ , which represents the mean dimension of crystallites perpendicular to planes  $hkl$ , can be evaluated from the Bragg's diffraction angle  $2\theta$  with the aid of the Sherrer equation<sup>22)</sup>:

$$L_{hkl} = \frac{5.73K\lambda}{\beta \cos \theta} \quad (\text{in nm}) \quad (1)$$

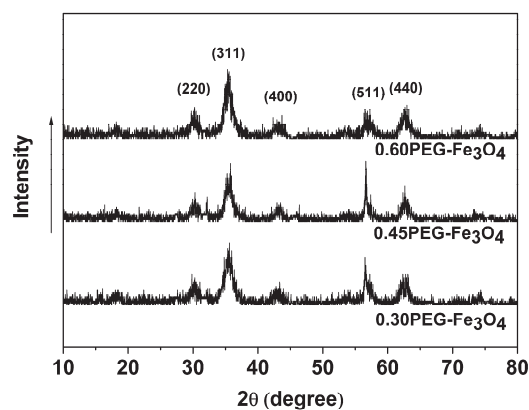


Fig. 2. X-ray diffraction patterns of the three kinds of PEG-coated Fe<sub>3</sub>O<sub>4</sub> nanoparticles as indicated.

Here,  $K$  ( $= 0.9$ ) is the shape factor,  $\lambda$  is the wavelength of incident X-ray, and  $\beta$  is the pure broadening profile (in unit of rad);  $\beta = \{B^2 - b_0^2\}^{1/2}$  with  $B$  and  $b_0$  (both in unit of rad) being the half-width of the measured profile and the instrumental broadening factor, respectively. The crystallite size of the PEG-coated  $\text{Fe}_3\text{O}_4$  nanoparticles thus evaluated,  $\cong 5.0$  nm, agrees well with the average nanoparticle size obtained from the TEM image ( $= 4$  nm; cf. Fig. 1).

### 3.3 FTIR Analysis

Fig. 3 shows the FTIR spectra of the three kinds of PEG-coated  $\text{Fe}_3\text{O}_4$  nanoparticles. For these nanoparticles, the characteristic adsorption band of  $\text{Fe}_3\text{O}_4$  magnetite at  $590\text{ cm}^{-1}$  is found but the other band of maghemite at  $630\text{ cm}^{-1}$  is not detected, confirming the purity of  $\text{Fe}_3\text{O}_4$  in these nanoparticles without further oxidation. Moreover, Fig. 3 also shows the C-O-C ether stretching and vibration bands at  $1065\text{ cm}^{-1}$  and  $1346\text{ cm}^{-1}$ , OH stretching/vibration band at around  $3400\text{ cm}^{-1}$ , C-H asymmetric/symmetric stretching and vibration band at  $2950\text{ cm}^{-1}$  and  $2860\text{ cm}^{-1}$ , respectively, which verifies the physical adsorption of PEG chains onto the  $\text{Fe}_3\text{O}_4$  nanoparticle surface.<sup>2, 14, 15)</sup>

### 3.4 Thermal Analysis

Fig. 4 illustrates the TGA curves of the three kinds of PEG-coated  $\text{Fe}_3\text{O}_4$  nanoparticles indicating the weight change of these nanoparticles with temperature ( $T$ ). With increasing  $T$ , the organic PEG component is completely decomposed to escape as a gas to convert the magnetite of the PEG-coated  $\text{Fe}_3\text{O}_4$  nanoparticles into pure iron oxides. Thus, the PEG coating layer physically adsorbed on the surface of  $\text{Fe}_3\text{O}_4$  nanoparticles can be characterized by the weight loss on heating. In Fig. 4, the first weight loss at around  $100$ - $150$  °C

(where PEG is chemically stable) is ascribed to evaporation of acetone (solvent utilized in synthesis of nanoparticles) remaining in the specimens, while the second weight loss at around  $230$ - $300$  °C is attributed to the decomposition of PEG. From the second weight loss, the PEG content was evaluated to be  $4.5$  wt%,  $5.2$  wt% and  $5.6$  wt% for the  $0.30\text{PEG-Fe}_3\text{O}_4$ ,  $0.45\text{PEG-Fe}_3\text{O}_4$  and  $0.60\text{PEG-Fe}_3\text{O}_4$  nanoparticles, respectively. Thus the PEG content increased with increasing amount of PEG in the feed solution utilized in the synthesis of nanoparticles.

### 3.5 Magnetorheological Behavior

#### 3.5.1 Overview

In general, under an external magnetic field, the magnetic nanoparticles aggregate to form clusters of the chain, column, or other complex shapes oriented in the field direction. This field-induced structural evolution of the PEG-coated  $\text{Fe}_3\text{O}_4$  nanoparticles (in the absence of shear flow) was observed with a digital microscope, and the results for the  $0.30$  PEG- $\text{Fe}_3\text{O}_4$  ferrofluids are shown in Fig. 5. The results for the  $0.45\text{PEG-Fe}_3\text{O}_4$  and the  $0.60\text{PEG-Fe}_3\text{O}_4$  ferrofluids were similar to those seen in Fig. 5.

In the PEG- $\text{Fe}_3\text{O}_4$  ferrofluids, the nanoparticles were well dispersed to form no large aggregates in the absence of the magnetic field, as confirmed from the digital microscopy (not shown here). Correspondingly, no aggregate was observed immediately after application of the magnetic field (panel a in Fig. 5). However, with increasing time up to  $180$  s (panels b, c, and d), the nanoparticles gradually moved under the magnetic field to aggregate into string-like clusters oriented in the field direction (indicated with the arrow). Note that the optically observed string-like structure is not a chain of the nanoparticles (having the average diameter of

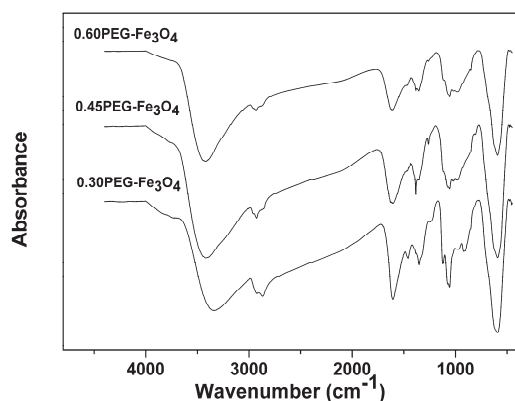


Fig. 3. FTIR spectra of the three kinds of PEG-coated  $\text{Fe}_3\text{O}_4$  nanoparticles as indicated.

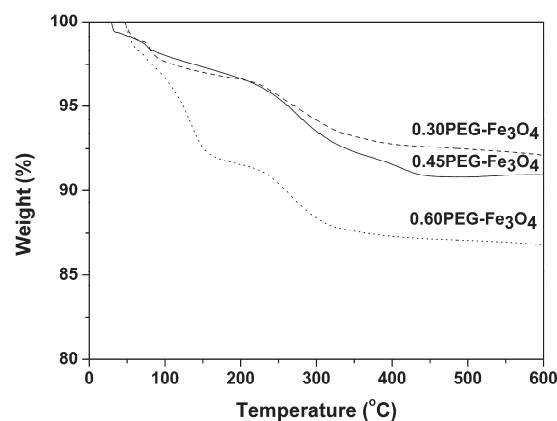


Fig. 4. Thermogravimetric analysis of PEG-coated  $\text{Fe}_3\text{O}_4$  nanoparticles as indicated.

4 nm) connected only in one dimension but a bundle-like cluster having an optically observable width. This structure formation results from the field-induced magnetic dipole in each nanoparticle and the resultant dipole-dipole interaction between the particles.

The magnetorheological property of the PEG-coated Fe<sub>3</sub>O<sub>4</sub> ferrofluids under steady shear was measured with a rotating rheometer in the parallel-plate geometry. The magnetic field was applied in the direction perpendicular to the plates (i.e., in the shear gradient direction). Fig. 6 shows plots of the steady state shear stress  $\sigma$  in the absence/presence of the magnetic field against the shear rate  $\kappa$ . The corresponding shear viscosity,  $\eta = \sigma/\kappa$ , is shown in Fig. 7. In the absence of the magnetic field, the ferrofluids behave essentially as a Newtonian fluid having a rate-insensitive viscosity (see filled squares in Fig. 7) because no large aggregates of the nanoparticles were formed therein. Under the magnetic field, the stress and viscosity increase because of the formation of the string-like clusters due to the field.

As can be noted in Fig. 6, the PEG-coated Fe<sub>3</sub>O<sub>4</sub> ferrofluids exhibit pseudo-plastic behavior under the magnetic field and this behavior at high shear rates  $\kappa \geq 20 \text{ s}^{-1}$  can be mimicked by the Bingham model giving a linear relationship between  $\sigma$  and  $\kappa$ ,

$$\sigma = \sigma_y + \eta_{pl}\kappa \quad (2)$$

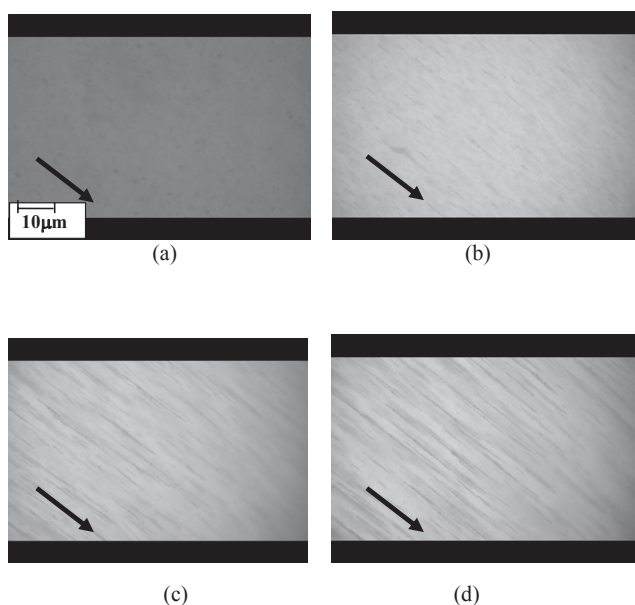


Fig. 5. The formation of cluster structures of 0.30PEG-coated Fe<sub>3</sub>O<sub>4</sub> nanoparticles in the direction of magnetic field indicated with the arrow. The time after application of the magnetic field was (a) 0 s; (b) 60 s; (c) 120 s; (d) 180s. Similar structural evolution was observed for 0.45PEG-coated and 0.60PEG-coated Fe<sub>3</sub>O<sub>4</sub> nanoparticles.

with  $\sigma_y$  and  $\eta_{pl}$  being the  $\kappa$ -independent yield stress and plastic viscosity, respectively. The  $\sigma_y$  and  $\eta_{pl}$  obtained by fitting the  $\sigma$  data of our ferrofluids at high  $\kappa$  ( $\geq 20 \text{ s}^{-1}$ ) with Eq.(2) are plotted against the magnetic flux density  $\psi$  in Figs 8 and 9, respectively. For ordinary magnetorheological fluids,  $\eta_{pl}$  is insensitive to  $\psi$  while  $\sigma_y$  is proportional to  $\psi^2$  in a considerably wide range of  $\psi$  (below a certain threshold). These features of  $\eta_{pl}$  and  $\sigma_y$  are a natural consequence of the invariance of  $\eta_{pl}$  and  $\sigma_y$  on reversal of the magnetic field direction (from  $\psi$  to  $-\psi$ ), as explained later in more details. In contrast, for our ferrofluids, the proportionality between  $\sigma_y$  and  $\psi^2$  cannot be clearly detected even at  $\psi < 0.1 \text{ T}$  (in a close vicinity of  $\psi = 0$ ); see dotted curves in Fig. 8. This result suggests that our ferrofluids do not have the real (static) yield stress that should be unequivocally proportional to  $\psi^2$  at least for  $\psi \rightarrow 0$ .

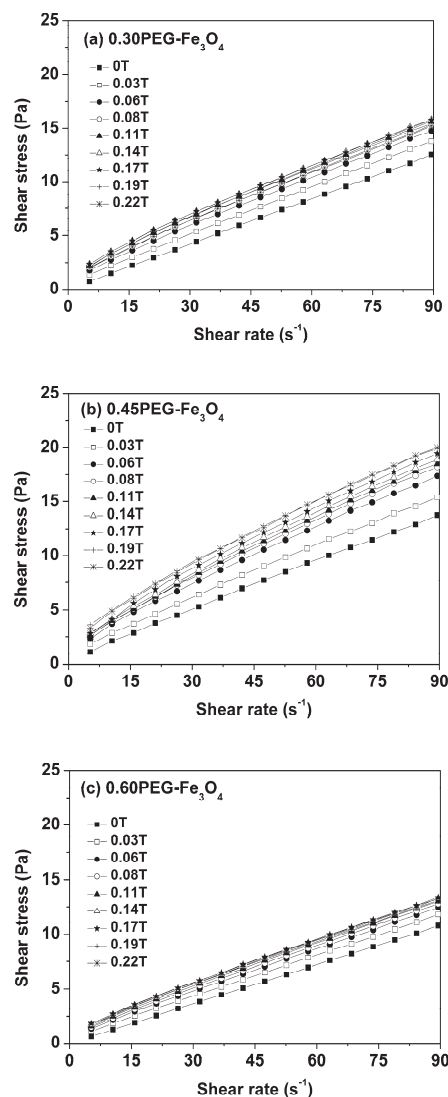


Fig. 6. Plots of steady state shear stress against shear rate for the PEG-coated Fe<sub>3</sub>O<sub>4</sub> ferrofluids under different magnetic flux densities: (a) 0.30PEG-Fe<sub>3</sub>O<sub>4</sub>; (b) 0.45PEG-Fe<sub>3</sub>O<sub>4</sub>; (c) 0.60PEG-Fe<sub>3</sub>O<sub>4</sub>.

The shear thinning of our ferrofluids (Figs 6 and 7) is superficially similar to that expected from Eq.(2). However, the decrease of the stress of those ferrofluids with decreasing shear rate  $\kappa$  is stronger than the linear decrease (down to  $\sigma_y$ ) expected from Eq.(2). Thus, we again confirm that our ferrofluids have practically no real yield stress, which means that the viscosity does not diverge even at the zero-shear limit. This behavior of our ferrofluids is in contrast to that of ordinary magnetorheological fluids, the latter obeying Eq.(2) down to the zero-shear limit and having the real yield stress due to huge column/string-like clusters connecting the measuring parts (plates) of the rheometer under the magnetic field. These huge clusters always reorganize themselves under the shear (due to the action of the magnetic field) to have the connectivity/size hardly changing with the shear

rate. Thus, under a given magnetic field, the rheological response of the huge clusters at non-zero shear is equivalent to that at the zero-shear limit, which results in the validity of Eq.(2) characterized by the real yield stress  $\sigma_y (\propto \psi^2)$  and  $\psi$ -insensitive  $\eta_{pl}$ . These  $\psi$  dependencies of  $\sigma_y$  and  $\eta_{pl}$  reflect shear-rate insensitivity of the huge cluster structure and the invariance of this structure on reversal of the magnetic field direction from  $\psi$  to  $-\psi$ . (The invariance of the structure on the field reversal, from  $\psi$  to  $-\psi$ , naturally requires  $\sigma_y$  and  $\eta_{pl}$  to be even functions of  $\psi$  and thus gives  $\sigma_y (\propto \psi^2)$  and  $\eta_{pl} (\propto \psi^0)$  for small  $\psi$ .)

As judged from the above features of ordinary magnetorheological fluids, the lack of the real yield stress in our ferrofluids suggests that the string-like clusters formed under the magnetic field are rather short and fragmented because the coating PEG layer disturbs real close contact of nanoparticles to weaken the inter-particles attraction under the magnetic field. In this consequence, the magnetorheological effect seen for our ferrofluids may be related to deformation/disruption of those short/fragmented clusters due to the shear

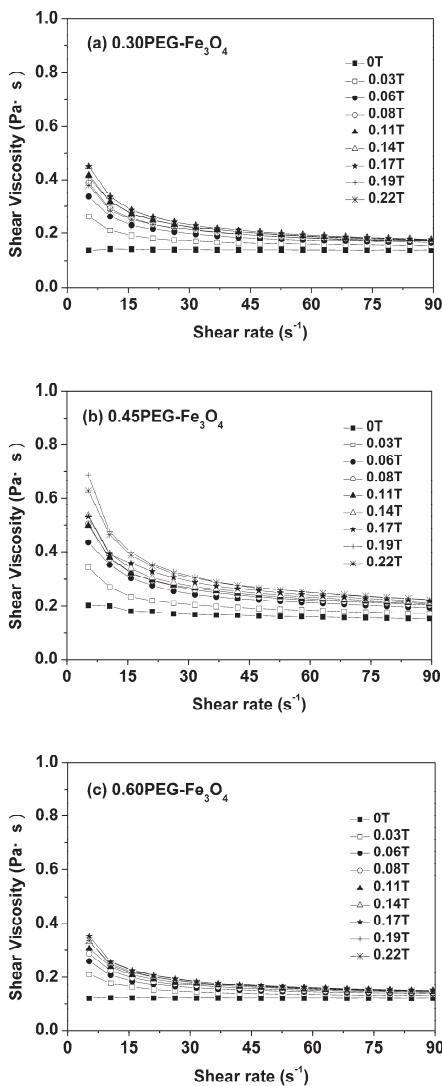


Fig. 7. Plots of steady state viscosity against shear rate for the PEG-coated  $Fe_3O_4$  ferrofluids under different magnetic flux densities: (a) 0.30 PEG- $Fe_3O_4$ ; (b) 0.45 PEG- $Fe_3O_4$ ; (c) 0.60 PEG- $Fe_3O_4$ .

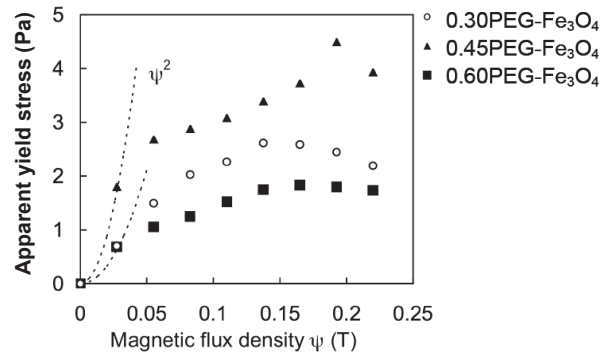


Fig. 8. Plots of apparent yield stress  $\sigma_y$  of the PEG-coated  $Fe_3O_4$  ferrofluids against magnetic flux density  $\psi$ . The dotted curved indicate a relationship,  $\sigma_y \propto \psi^2$ .

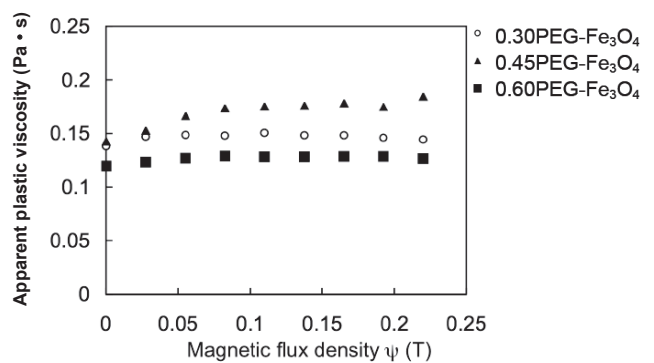


Fig. 9. Plots of apparent plastic viscosity  $\eta_{pl}$  of the PEG-coated  $Fe_3O_4$  ferrofluids against magnetic flux density  $\psi$ .

flow: The clusters would be more stabilized under a stronger magnetic field, which results in a larger mechanical energy required to deform/disrupt the clusters. Correspondingly, the stress/viscosity corresponding to this energy increases under the magnetic field; namely, the magnetorheological effect emerges. In this sense, this effect in our ferrofluids appears to be similar to the enhancement of the pseudo-plastic behavior of ordinary suspensions (under no magnetic field) that contain finite-sized aggregates of particles: As the aggregates become more stabilized, the energy required to deform/disrupt the aggregates becomes larger to give this enhancement.

### 3.5.2 Effect of PEG-coating on rheological behavior of ferrofluids

*In the absence of the magnetic field*, the stress/viscosity firstly increases with increasing amount of the PEG coating (from the 0.30PEG-Fe<sub>3</sub>O<sub>4</sub> ferrofluid to the 0.45PEG-Fe<sub>3</sub>O<sub>4</sub> ferrofluid) but then decreases on a further increase of this amount (to the 0.60PEG-Fe<sub>3</sub>O<sub>4</sub> ferrofluid), as can be noted in Figs 6 and 7. This non-monotonic change suggests that our ferrofluids have at least two contributions to the measured stress, the stress due to inter-particle potential (that emerges even in the absence of close contact of particles) and the stress due to relaxation of PEG chains in the coating layer (swollen with the oligomeric PEG solvent).<sup>23)</sup>

The inter-particle potential force in our ferrofluids should be rather short-ranged, as typically known for aggregating suspensions. In addition, the coating layer should increase its thickness and become concentrated with increasing amount of PEG chains therein, which would retard the motion of those chains and enhance the PEG chain contribution to the stress.<sup>23)</sup> Thus, we expect that the inter-particle potential force does not decrease significantly on a small increase of the PEG content but the stress due to PEG chains in the coating layer increases because of the increase of concentration and the retardation of the PEG chain motion. These changes could result in the increase of the stress/viscosity from 0.30PEG-Fe<sub>3</sub>O<sub>4</sub> to 0.45PEG-Fe<sub>3</sub>O<sub>4</sub>. A further increase of the PEG content (from 0.45PEG-Fe<sub>3</sub>O<sub>4</sub> to 0.60PEG-Fe<sub>3</sub>O<sub>4</sub>) could result in the increase of the PEG layer thickness beyond a critical thickness, and the corresponding decrease of the inter-particle stress could overwhelm the increase of the stress due to PEG chains. The decrease of the stress/viscosity from 0.45PEG-Fe<sub>3</sub>O<sub>4</sub> to 0.60PEG-Fe<sub>3</sub>O<sub>4</sub> may reflect this situation.

Now, we turn our focus to the contribution of PEG layer to the magnetorheological effect of the ferrofluids. For discussion of this effect, we should first note the behavior in the absence of the magnetic field: Ordinary nano-ferroparticles having no PEG coating layer usually form huge aggregates, while our

PEG-coated nano-ferroparticles do not. Thus, the PEG layer on our particles should give a repulsive (steric) barrier that cannot be overcome by the particle thermal energy of order of  $k_B T$  ( $k_B$  = Boltzmann constant,  $T$  = absolute temperature) thereby stabilizing the particle dispersion. In contrast, the magnetic force brings the PEG-coated particles into close contact and leads to the cluster (aggregate) formation seen in Fig. 5. This force should be associated with the magnetic energy well above  $k_B T$  (otherwise, the clusters would not be stabilized). Then, in the clusters, the PEG layer on the particles should be mutually squeezed to overlap to some extent. This overlapping of the PEG layers in the clusters is the key in the following discussion.

As can be noted from Figs. 6 and 7, magnetorheological effect at low shear rate  $\kappa$  is larger in the order, 0.45PEG-Fe<sub>3</sub>O<sub>4</sub> > 0.30PEG-Fe<sub>3</sub>O<sub>4</sub> > 0.60PEG-Fe<sub>3</sub>O<sub>4</sub>. This fact can be related to the mechanism of the magnetorheological effect discussed earlier, the flow-induced deformation/disruption of short clusters formed under the magnetic field. The nanoparticles may aggregate less densely and the resulting clusters are less stabilized when the PEG coating layer becomes thicker to prevent close contact of the nanoparticles, which results in a decrease of the stress required for deformation/disruption of the clusters. On the other hand, the relaxation of the PEG chains in the particle-coating layers overlapping in the clusters is retarded more strongly when the PEG layer becomes more concentrated and thicker, which enhances the stress for deformation/disruption of the clusters. The magnitude of the magnetorheological effect observed for our ferrofluids would be determined by a trade-off of these contradicting changes of the stress with the PEG layer thickness, possibly becoming the largest for the intermediate PEG content (0.30PEG-Fe<sub>3</sub>O<sub>4</sub>).

For ordinary, aggregating suspensions under no magnetic field, the decrease of the cluster size with increasing shear rate results in the pseudo-Bingham behavior. The deviation from Eq.(2) seen for our ferrofluids seems to be similar to this behavior of ordinary suspensions, although the clusters in the ferrofluids are formed because of the action of the magnetic field. This argument is consistent with the observation that the stress/viscosity of our three ferrofluids at high shear rate almost coincide with each other and approach those of the fluids under no magnetic field; see Figs 6 and 7. As judged from this coincidence, the cluster size in our ferrofluids under the magnetic field would have decreased with increasing shear rate and the clusters appear to have been almost fully disrupted by the high shear examined. This disruption of the clusters should have contributed, at least partly, to the deviation from the Bingham Eq.(2) explained earlier. Thus,

these arguments are consistent with the magnetorheological behavior of the ferrofluids. However, no structural evidence has been obtained. This observation, under the shear and magnetic fields, is now being attempted.

#### 4. CONCLUSIONS

In this paper, three kinds of PEG-coated Fe<sub>3</sub>O<sub>4</sub> nanoparticles carrying different amount of PEG were synthesized and the magnetorheological properties were examined for ferrofluids (suspensions) of these nanoparticles in a oligomeric PEG-400. The PEG coating physically adsorbed on the nanoparticle surface was confirmed from FTIR and TGA analysis. The introduction of the PEG coating did not affect the crystalline structure of Fe<sub>3</sub>O<sub>4</sub> (as confirmed from X-ray diffraction) but enhanced uniform dispersion of the nanoparticles (no large aggregates were found in microscopy observation in the absence of the magnetic field). The ferrofluids essentially behaved as Newtonian fluids in the absence of the magnetic field, which naturally reflected this lack of large aggregates. However, under the magnetic field, the shear stress/viscosity increased because of formation of string-like clusters of nanoparticles oriented in the field direction. Differing from ordinary magnetorheological fluids, our ferrofluids did not have a real (static) yield stress probably because the clusters formed therein were short/fragmented and not connecting the measuring parts (plates) in the rheometer. This fact in turn suggested that the magnetorheological effect seen for our ferrofluids corresponded to the flow-induced deformation/disruption of those short clusters.

#### Acknowledgements

This research was supported by the National Natural Science Foundation of China (No. 20803047), the Chen Xing Young Scholar Award Program of Shanghai Jiao Tong University (No. T241460617), Shanghai Undergraduate Innovative Activity Program (No. IAP2033), and partly by Grant-in-Aid for Scientific Research on Priority Area "Soft Matter Physics" from the Ministry of Education, Culture, Sports, Science and Technology, Japan (No. 18068009). The authors also thank Instrumental Analysis Center of Shanghai Jiao Tong University for the assistance with the measurements.

#### REFERENCES

- 1) KHerv'e, Douziech-Eyrolles L, Munnier E, Cohen-Jonathan S, MSouc'e, HMarchais, Limelette P, Warmont F, Saboungi ML, Dubois P and Chourpa I, *Nanotechnology*, **19**, 465608 (2008).
- 2) Feng B, Hong RY, Wang LS, Guo L, Li HZ, Ding J, Zheng Y, Wei DG, *Colloids and Surfaces A: Physicochem Eng Aspects*, **328**, 52 (2008).
- 3) Chertok B, Moffat BA, David AE, Yu FQ, Bergemann C, Ross BD, Yang VC, *Biomaterials*, **29**, 487 (2008).
- 4) Zhang LY, Gu HC, Wang XM, *J Magn Magn Mater*, **311**, 228 (2007).
- 5) Hergt R, Dutz S, *J Magn Magn Mater*, **311**, 187 (2007).
- 6) Alexiou C, Arnold W, Klein RJ, Parak FG, Hulin P, Bergemann C, Erhardt W, Wagenpfeil S, Lübke AS, *Cancer Res*, **60**, 6641 (2000).
- 7) Son SJ, Reichel J, He B, Schuchman M, Lee SB, *J Am Chem Soc*, **127**, 7316 (2005).
- 8) Kaufman CL, Williams M, Ryle LM, Smith TL, Tanner M, Ho C, *Transplantation*, **76**, 1043 (2003).
- 9) Berry CC, Wells S, Charles S, Aitchison G, Curtis AS, *Biomaterials*, **25**, 5405 (2004).
- 10) Zhang Y, Kohler N, Zhang M, *Biomaterials*, **23**, 1553 (2002).
- 11) Butterworth MD, Illum L, Davis SS, *Colloids Surf A*, **179**, 93 (2001).
- 12) Xie J, Xu C, Kohler N, Hou Y, Sun S, *Adv Mater*, **19**, 3163 (2007).
- 13) Mondini S, Cenedese S, Marinoni G, Molteni G, Santo N, Bianchi CL, Ponti A, *J Colloid Interface Sci*, **322**, 173 (2008).
- 14) Zhang Y, Kohler N, Zhang MQ, *Biomaterials*, **23**, 1553 (2002).
- 15) Peng J, Zou F, Liu L, Tang L, Yu L, Chen W, Liu H, Tang JB, Wu LX, *Trans Nonferrous Met Soc China*, **18**, 393 (2008).
- 16) D'Souza AJ, Schowen RL, Topp EM, *J Controlled Release*, **94**, 91 (2004).
- 17) Nishiyama H, Katagiri K, Hamada K, Kikuchi K, *Int J Modern Phys B*, **19**, 1437 (2005).
- 18) Wang XJ, Gordaninejad F, *Rheol Acta*, **45**, 899 (2006).
- 19) See H, Chen R, *Rheol Acta*, **43**, 175 (2004).
- 20) Laun HM, Gabriel C, Schmidt G, *J Non-Newtonian Fluid Mech*, **148**, 47 (2008).
- 21) Ge J, Hu Y, Biasini M, Dong C, Guo J, Beyermann WP, Yin Y, *Chem Euro J*, **13**, 7153 (2007).
- 22) Alexander LE, "X-ray diffraction methods in Polymer science", Wiley-Interscience, New York, 1969.
- 23) Hong RY, Zhang SZ, Han YP, Li HZ, Ding J, Zheng Y, *Powder Technology*, **170**, 1 (2006).